Technical Report

Department of Computer Science
and Engineering
University of Minnesota
4-192 Keller Hall
200 Union Street SE
Minneapolis, MN 55455-0159 USA

TR 16-032

Mapping Burned Areas in Tropical forests using MODIS data

Varun Mithal, Guruprasad Nayak, Ankush Khandelwal, Vipin Kumar, Ramakrishna Nemani, Nikunj C. Oza

September 2, 2016

Revised

Mapping Burned Areas in Tropical forests using MODIS data

Varun Mithal[1], Guruprasad Nayak[1], Ankush Khandelwal[1], Vipin Kumar[1], Ramakrishna Nemani[2] and Nikunj C. Oza[2]

[1]Department of Computer Science, University of Minnesota*

[2]NASA Ames Research Center†

Abstract

This paper presents a new burned area product for the tropical forests in South America and South-east Asia. The product is derived from Moderate Resolution Imaging Spectroradiometer (MODIS) multispectral surface reflectance data and Active Fire hotspots using a novel rare class detection framework that builds data-adaptive classification models for different spatial regions and land cover classes. Burned areas are reported for 9 MODIS tiles at a spatial resolution of 500 m in the study period from 2001 to 2014. The total burned area detected in the tropical forests of South America and South-east

*(mithal,nayak,ankush,kumar)@cs.umn.edu

†(rama.nemani,nikunj.c.oza)@nasa.gov

Asia during these years is 2,286,385 MODIS pixels (approximately 571 K sq. km.), which is more than three times compared to the estimates by the state-of-the art MODIS MCD64A1 (742,886 MODIS pixels). We also present validation of this burned area product using (i) manual inspection of Landsat false color composites before and after burn date, (ii) manual inspection of synchronized changes in vegetation index time series around the burn date, and (iii) comprehensive quantitative validation using MODIS-derived differenced Normalized Burn Ratio (dNBR). Our validation results indicate that the events reported in our product are indeed true burn events that are missed by the state-of-art burned area products.

Keywords: MODIS, Burned Area Mapping, Tropical forests

1 Introduction

Forest fires are known to generate a significant flux of greenhouse gases and particulate matter into the atmosphere and also contribute to several ecological effects such as the loss of animal habitat and biodiversity (Minko (2000)). In the tropical forests, fires are often associated with active deforestation fronts and linked to illegal establishment of industrial timber, oil palm, soy, and tea and coffee plantations (Fuller and Fulk (2001)). Forest fire mapping from satellite data offers opportunities for providing timely information on the implementation of sustainable forest management, which is critical for making sound policy decisions for protecting forests. Furthermore, multi-annual burned area products are also needed to improve the understanding

of the relationship between climate, vegetation and fires (Chen et al. (2011)). As a result, there has been an increase in demand for automated and reliable tools to monitor forest fires from earth observing satellite data (Randerson et al. (2012)).

Existing satellite-based techniques for burn area assessment can be grouped into two broad categories- active fire (hotspot) detection and post-fire burned area mapping. Hotspot detection approaches use thermal energy associated with burning of biomass to map active (ongoing) fires with the purpose of real-time fire management. A number of papers have used active fire data as a proxy to report the burned area estimates (Schultz (2002), Smith et al. (2007), Sukhinin et al. (2004)). However, hotspot detection methods are known to have a high omission error rate because they tend to miss burned pixels due to obstruction by clouds and smoke as well as due to limited satellite diurnal sampling (i.e. satellite overpass occurred when the fires were not burning) (Giglio et al. (2009)). Moreover, active fire often overestimates burned area in regions with a large proportion of small, sub-pixel fires (Fraser et al. (2000)). In contrast, post-fire burned area mapping techniques consider satellite observations of the land surface over a longer temporal interval around the burn date to create more reliable historical maps of burned areas (Giglio et al. (2009), Loboda and Csiszar (2007), Pu and Gong (2004), Pu et al. (2004), Roy et al. (1999)). Note that post-fire mapping techniques are relatively more robust to issues due to cloud cover or smoke from fires because often burn scars remain detectable in the spectral observations for several months after the burn date. This paper presents a new post-fire burned area product for tropical forests derived from MODIS Surface Reflectance 8-day

composite product (Vermote et al. (2011)) and MODIS active fire product (Giglio et al. (2006)).

Satellite-based post-fire burned area mapping algorithms face two key challenges. First, the relationship between the explanatory variables (spectral features) and target variable (burned/unburned) changes with spatial regions and land cover (Giglio et al. (2009)). Therefore, learning a single classification model to distinguish burned pixels from unburned pixels and applying it across different land cover classes and geographies can have a poor performance. One approach to address this issue is to train separate customized models for each land cover and spatial region. However, this requires annotated training samples in each land cover and geographical region, which is infeasible due to the considerable human effort involved in collecting training samples using ground and aerial surveys. Hence, existing approaches make use of active fire hotspots to select the training samples for burned and unburned classes (Fraser et al. (2000), Giglio et al. (2009)). But active fire hotspots are only imperfect surrogates for burned areas; therefore, previous studies use hand-crafted "cleaning" rules while selecting training pixels from active fire hotspots to ensure that the training samples are accurate. As an example, Giglio et al. (2009) restrict burned samples to those in which the value of normalized change in vegetation index exceeds 2. But, the spectral diversity of burned pixels can make such "cleaning heuristics" used for selecting training samples very brittle in some regions. Second, the problem of identifying fires differs from traditional classification problems because of the extreme class imbalance, i.e. the unburned locations considerably outnumber the burned locations. Thus, even a small false positive rate can result

in a significant number of spurious burned areas (Senator (2005)). To avoid this issue, existing methods tend to use hand-crafted rules that maintain a very low rate of commission errors. Note that these hand-crafted rules and parameters used for selecting training pixels from active fire hotspots and for constraining the number of spurious burn detections in existing algorithms are selected empirically by experts based on their performance in ecosystems where some annotated training data is available (Bastarrika et al. (2011)). We notice that these parameters are perhaps too conservative for the tropics. As a result, existing products tend to detect only the more clearly burned pixels in the tropics, at the cost of omitting many burned pixels.

We address these issues using a three stage framework- RAre class Prediction in the absence of True labels (referred to as RAPT). The RAPT framework is able to automatically adapt model parameters as the relationship between the explanatory and target variable changes with spatial region and land cover class without any hand-crafted heuristics for obtaining clean training samples. The first stage of RAPT assigns each pixel a burn scar label (yes/no) by building a classifier on MODIS multispectral surface reflectance. Training samples are selected by using a random sample of active fire hotspots as burned training samples and a random sample of other pixels as unburned. To minimize the impact of inaccuracies in the positive and negative training samples, a new learning framework is used in Stage 1 that has been shown to be robust to noise in training labels under certain assumptions (Mithal et al. (2016)). In fact, the accuracy of classifiers trained on noisy training samples has been shown to be nearly as good as the one of classifiers trained on samples obtained using high quality fire perimeters that are avail-

able for several states in the United States (Mithal et al. (2016)). Stage 1 of RAPT also addresses the trade-off between omission and commission errors in a principled manner by automatically selecting the classification model parameters that jointly maximize the user's and producer's accuracy of the burned class. Note that despite a low false positive rate at the end of stage 1, the user's accuracy for the burned class can still be quite poor due to the extreme imbalance between the burned and unburned classes. The second stage of RAPT uses co-occurrence of Active Fire hotspots and burn scar to identify confident burns, which will have a lower commission error rate than both Active fire hotspots and burn scars individually. These confident burns are unlikely to be spurious events, as the probability of the two sources- active fire and scar classifier- making an error at the same location tends to be low. However, the reduction in errors of commission is achieved at the cost of increasing the errors of omission. The third stage of RAPT uses spatial context to improve the coverage of burned areas in the spatial proximity of the confident burns identified in the second stage. In particular, this stage includes pixels with burn scars that are connected to confident burned areas as part of the final event, even though they do not have an active fire present. The spatial connectivity constraint ensures that the coverage of final RAPT burned areas is increased without including many spurious detections.

The RAPT framework was applied in the tropical forests in Amazon and South-east Asia between the years 2001-2014 and identified 2,286,385 MODIS pixels (approximately 571 K sq. km.), which is three times more than the burned area estimated by the commonly used MCD64A1 product (Giglio et al. (2009)). In this paper, we also present three lines of evidence to validate

the events reported in RAPT product. First, we manually examined Landsat false color composite images before and after the burn dates for a sample of reported events for which cloud free images were available close to the date of the event. Our results indicate that the RAPT events show a visible burn scar in their after-burn composite images. Second, manual inspection of the enhanced vegetation index (EVI) time series of the pixels that are part of RAPT events shows that a large number of these time series have an abrupt loss in vegetation on the event date reported by RAPT algorithm followed by a gradual recovery, which is the expected behavior from burned pixels. Moreover, we observed that the changes occurring in EVI are synchronized in time (around the event date) for the locations that are part of the same RAPT event, increasing our confidence that these locations had a fire at the event date, since fires tend to burn nearby locations in a short time interval. Finally, a comprehensive quantitative evaluation using MODIS-derived differenced Normalized Burn Ratio (dNBR) (Loboda et al. (2007)) was done to estimate the user's and producer's accuracy of the fire events. These validation results increase our confidence that the events reported in RAPT product are indeed burn events.

We have created a publicly accessible web-based viewer for visualizing our burned area product `http://arizona-umh.cs.umn.edu/FireMonitorRelease/`. The viewer shows the RAPT events corresponding to a user-selected MODIS tile and year as event polygons. Polygon-level statistics such as total number of MODIS pixels, number of pixels with an active fire hotspot, and the number of pixels identified by MCD64A1 are reported. The MODIS pixels belonging to a particular event polygon can also be viewed by selecting the

polygon. In addition, relevant information about these MODIS pixels (such as their Enhanced Vegetation index series, Normalized Burn Ratio index series, and MODIS land cover classification labels) can be queried by selecting (clicking) one of the pixels.

2 Burned Area Detection Method

2.1 Study area and input data

This study considers the burned areas in forests located in tropical regions in South America and South-east Asia. The burned area detection algorithm uses the 500 m MODIS Surface Reflectance 8-day composite product (Vermote et al. (2011)) (https://lpdaac.usgs.gov/dataset_discovery/modis/modis_products_table/mod09a1) , MODIS active fire product (Giglio et al. (2006)) (https://lpdaac.usgs.gov/dataset_discovery/modis/modis_products_table/mod14a2) , and MODIS MOD12Q1 land cover classification product (Friedl et al. (2002)) (https://lpdaac.usgs.gov/dataset_discovery/modis/modis_products_table/mcd12q1) . The MODIS products are defined on global sinusoidal grids in fixed geolocated tiles approximately 10 degree by 10 degree in size and are publicly available from Land Processes Distributed Active Archive Center. Landsat ETM+ scenes are used in this study for validating a sample of the RAPT fire events by manual inspection. Moreover, MODIS MCD64A1 (Giglio et al. (2009)) (http://modis-fire.umd.edu/pages/BurnedArea.php?target=Download) is used as an existing state-of-art burned area product for comparative study.

2.2 The RAPT framework

Our burned area detection framework is designed to combine the information in MODIS active fire hotspots and multispectral surface reflectance data for global-scale burned area detection. The detection algorithm proceeds through the three stages described below (Figure 1 shows flowchart of the RAPT framework).

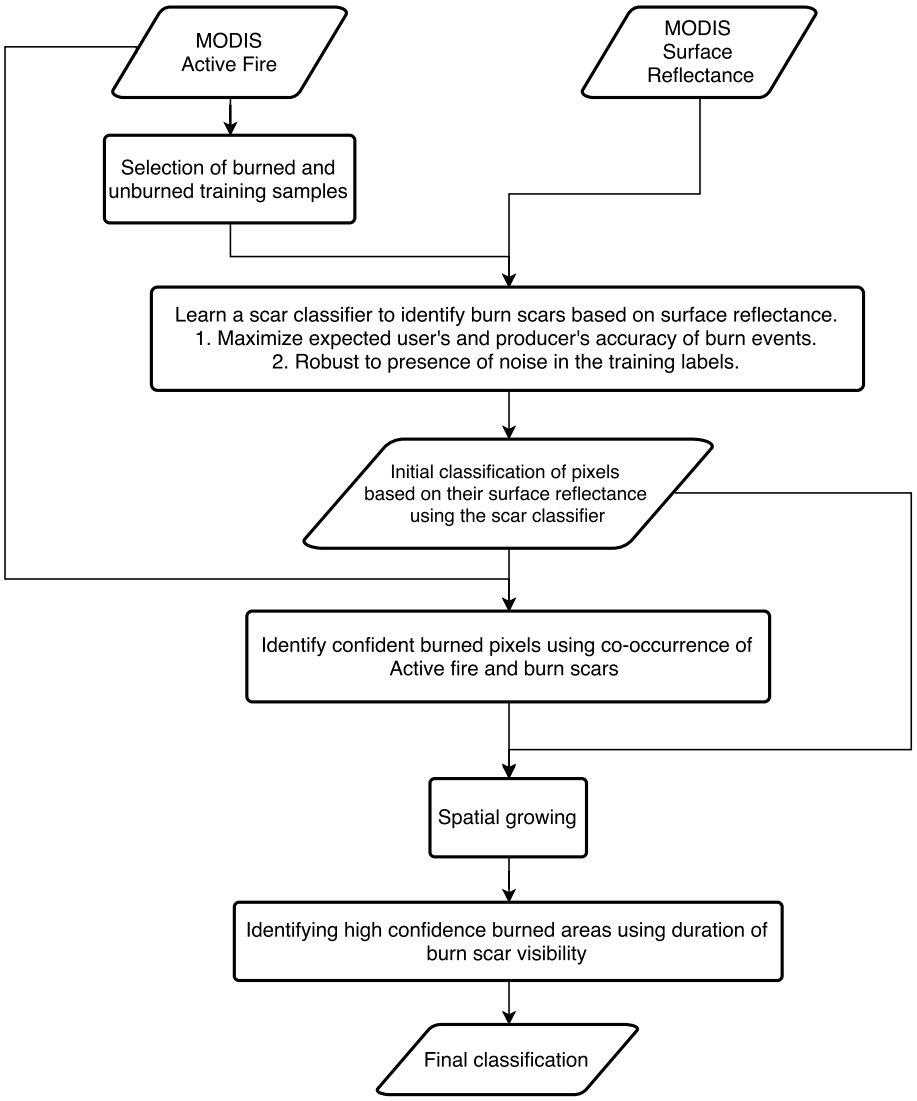

Figure 1: Flowchart showing the steps of the RAPT framework

2.2.1 Stage 1: Identifying burn-scars from spectral data

In this step a classification model is trained to identify the pixels with a burn-scar based on their surface reflectance observations. This classifier is then applied on all instances to produce the initial classification for each 500 m pixel at every time step. Pixels identified by this classifier are treated as *candidate burned pixels*, which are then refined in the subsequent stages to give the final burned areas. The classifier uses MODIS multispectral surface reflectance 8-day composite product for identifying the burn-scars. Specifically, the classification model to separate burned pixels from unburned pixels is trained on a 7-dimensional feature space consisting of all the seven bands of MODIS multispectral reflectance data. This stage requires selection of training samples and building a classification model using the samples.

Selecting training pixels We make use of the active fire hotspots to select the training samples for burned and unburned classes to train the scar classifier. In particular, we select active fire pixels as training samples for burned class if they form a spatial cluster of size greater than 10 pixels. This spatial pruning is done to eliminate active fire pixels belonging to sub-pixel burns. Pixels with an active fire observation on a given date are more likely to show a burn scar than those without an active fire. However, active fire hotspots are only a weak surrogate for burn-scars and a training data set created using active fire observations is often contaminated with noise in the labels of the training samples.

Building classification model with noisy training samples We use a logistic regression model as our classifier (Koutsias and Karteris (1998)). It models the probability that a pixel with spectral observation $\mathbf{x}$ belongs to the burned class as a logistic sigmoid acting on a linear function of $\mathbf{x}$,

$$P[y = 1|\mathbf{x}; \mathbf{w}] = \sigma(\mathbf{w}^T\mathbf{x})$$

where the logistic sigmoid function is defined as $\sigma(z) = 1/(1+e^{-z})$. The final classifier is written in the following form: $y = 1$ if $P[y = 1|\mathbf{x}; \mathbf{w}] \geq \gamma$ and 0 otherwise. The threshold γ determines the trade-off between the errors of omission and commission, which varies as γ is swept from 0 to 1. In case of burned area mapping a suitable classification objective is to jointly maximize the user's accuracy and producer's accuracy of the burned class. Therefore, in the RAPT framework we select γ to maximize the product of user's accuracy and producer's accuracy of the burned class. Note that selecting the decision threshold γ by maximizing the product of the user's and producer's accuracy ensures that the errors of omission and commission are relatively balanced.

A gradient descent algorithm is used to select the model parameters w of the logistic regression model. This logistic regression model is then used to estimate the conditional probability $P[y = 1|\mathbf{x}; \mathbf{w}]$ for every pixel. The selection of decision threshold γ is a challenge in our problem setting because the training data created using active fire hotspots is plagued with noise in training labels, therefore estimation of user's and producer's accuracy corresponding to different choices of γ is tricky. In particular, if we ignore the noise in labels of training samples, it may lead to incorrect estimation of user's

and producer's accuracy resulting in selection of a sub-optimal threshold value, due to which the classification model will show higher rates of omission and commission compared to the optimal model. To address this issue we use a new learning procedure (Mithal et al. (2016)), which is especially designed to build classification models when training samples suffer from label noise in the context of imbalanced class problems such as burned area mapping. This new learning algorithm allows us to use active fire hotspots as a surrogate of burned areas for training classifier to identify burn-scar without incurring any additional cost of annotating training samples. In fact, Mithal et al. (2016) shows, both theoretically and empirically, that the performance of the classifier trained on training samples selected using active fire is expected to be similar to the performance of the classifier trained using gold standard training samples of burned and unburned pixels.

Note that it is possible that the scar classifier built in stage 1 has a poor user's accuracy, especially if the burned and unburned samples are not separable in the feature space. Burned area detection in such regions and land cover classes may lead to poor user's accuracy, and hence it may be desirable to skip detection in these regions to avoid too many false positives. In fact, some existing burned area algorithms use a form of separability test to decide whether a good classifier can be built for a given region and land cover. For example, Giglio et al. (2009) used a measure of separability between the distribution of vegetation differences of burned and unburned samples to determine if their burned area algorithm is to be applied to the region. Since the objective is to achieve high user's accuracy, we use an estimate of the user's accuracy of the burned areas identified in stage 1 as a

measure of separability of the burned and unburned class. Though it is not possible to estimate user's accuracy without access to gold standard labels, the analysis presented in Mithal et al. (2016) shows that it is possible to estimate a lower bound on user's accuracy of stage 1. We use this lower bound as our test of separability, and execute RAPT on a tile only if the estimated lower bound is greater than a pre-specified threshold (10% was used in this study).

2.2.2 Stage 2: Identifying confident burned pixels

In the second stage, each pixel is classified as either confident burn or unlabeled by combining the predictions of the scar classifier and the active fire hotspots. We use a conservative combination step that labels a pixel as confident burn if it is identified both by the scar classifier and active fire. As a result, confident burn pixels exhibit both burn-scars and thermal anomaly signals. This strict criterion ensures that the confident burn pixels have a smaller number of commission errors compared to both the scar classifier and active fire hotspots individually.

2.2.3 Stage 3: Spatial growing and final classification

The confident burned areas, identified in the previous step, typically cover only a small fraction of the total burned pixels. This is especially true in the tropics where active fire hotspots have a low coverage due to poor data quality (eg. obstruction by clouds) and limited frequency of satellite overpass. Therefore, in the third step of RAPT we improve the coverage of burned areas by leveraging the spatial context of confident burned pixels and candidate

burned pixels. More specifically, a *spatial growing* method is used, which includes the pixels that show a burn-scar but are not detected as confident burns as part of final burned areas if they are spatially connected to some confident burned pixels within a spatial distance of 5 MODIS pixels. This is a manually selected threshold, but the performance is not very sensitive to it. In fact, our experimental results indicated that if we choose the distance threshold between 5 to 10 pixels, the results remained unchanged for most tiles and years. However, having this threshold as low as 5 is helpful in ensuring that large spatial regions incorrectly classified as burned in Stage 1 do not get classified as burned at the end of Stage 3 just due to a spurious active fire hotspot that coincides with the onset of event in Stage 1.

Finally, we use temporal persistence as a measure of confidence for detected events and reduce spurious detections. In most fires burn scars remain visible for multiple time steps, and RAPT uses the length of the temporal window for which the scar is visible as a measure of the confidence of the burn event. In this paper, we report burn events for which the scar was visible for at least 4 time steps (i.e. a month). Note that one can potentially use a lower confidence RAPT burned area product that includes detected events with a smaller scar window of 1-3 time steps. However, including the low confidence events will increase the number of commission errors.

Land cover and geographical partitioning To account for the spectral diversity of burn scars, we train multiple classification models, each focusing on a smaller, homogeneous partition of the data, grouped according to the land cover class and geographical region. Learning a separate, customized

classifier for each homogeneous group is known to improve the burned area detection performance, as it allows for automated adaptation of model parameters to the specifics of fire occurrence in the biome and spatial region of interest (Giglio et al. (2009)). Specifically, in our detection framework, we create separate groups corresponding to each MODIS tile (to address geographical heterogeneity) and each MODIS land cover class (to address land cover heterogeneity).

Moreover, burned area results are reported for only stable forest pixels. A pixel is considered to belong to stable forest in a particular year if it is labeld as forest by MODIS land cover in the previous year as well as in the first 4 years (i.e., 2001-2004).

3 Burned Area Detection in Tropical forests

The RAPT framework is applied to the forested locations in 15 MODIS tiles in South America and South-east Asia between 20°N and 20°S latitudes from 2001 to 2014. We report results only for 9 of these MODIS tiles, as for the other 6 tiles RAPT stage 1 classifier did not pass the separability test, i.e. the estimated lower bound on the user's accuracy was below the specified threshold of 10%. These excluded tiles appear to have much less fire activity than other tiles since they account for less than 10% of the total number of burned locations found by MCD64A1 in the 15 tiles.

In the following, we compare the burned area estimates by RAPT to MCD64A1, which is a widely used global-scale post-fire burned area product. For ease of comparison we scaled RAPT and MCD64A1 to annual

Table 1: Table reports the number of burned pixels (at 500 m. spatial resolution) corresponding to RAPT (only), Common and MCD64A1 (only) for each tile in the region of study.

MODIS tile	RAPT only	Common	MCD64A1 only
h11v09	319956	45108	11923
h12v09	542753	126040	17042
h11v10	266256	100025	59523
h12v10	235814	138924	75873
h13v09	152867	14957	1587
h28v08	72978	16184	16193
h29v08	331139	2167	10441
h28v09	52567	17084	18796
h29v09	106667	42899	28120
Total	1782997	503388	239498

products, i.e. every year each 500 m pixel in the product was assigned to either burned or unburned class depending on whether it is flagged as burned in at least one of the dates in the corresponding year. On comparing the two products for a given year, each pixel belongs to one of the following categories- reported as burned by both products, reported as burned only by RAPT and unburned by MCD64A1, reported as burned only by MCD64A1 and unburned by RAPT, or reported as unburned by both products. Table 1 reports the number of burned pixels belonging to each of the three categories- RAPT (only), Common (i.e. both RAPT and MCD64A1), and MCD64A1 (only) aggregated over the 14 years. We observe that RAPT identifies about 67% of burned areas reported by MCD64A1. But more importantly, RAPT identifies 2,286,385 MODIS pixels (approximately 571 K sq. km.), which is about three times as many burned areas compared to MCD64A1.

4 Validation of RAPT events

Rigorous validation of any global burned area data set requires independent, gold standard maps of burned areas for different regions of study. To the best of our knowledge, no such high quality comprehensive maps are available for the tropical forests. Therefore, we looked at multiple independent sources of evidence to validate the burned areas detected by RAPT. These included: (1) manual inspection using medium resolution Landsat false color composites, (2) manual inspection using vegetation index time series, and (3) comprehensive quantitative validation using the difference in Normalized Burn Ratio (dNBR) computed from pre-event and post-event MODIS multispectral reflectance images. The goal of these validation studies is to show that the events reported by RAPT are indeed true burns. For a more thorough validation, we have made our product available publicly by a web-based viewer `http://arizona-umh.cs.umn.edu/FireMonitorRelease/`.

4.1 Manual inspection using Landsat images

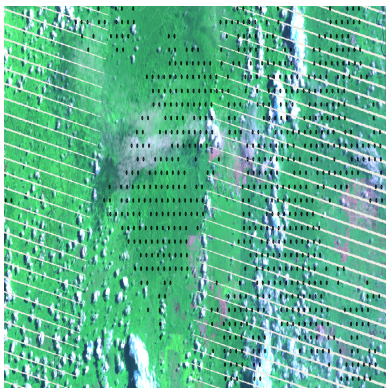

(a) Before fire event.

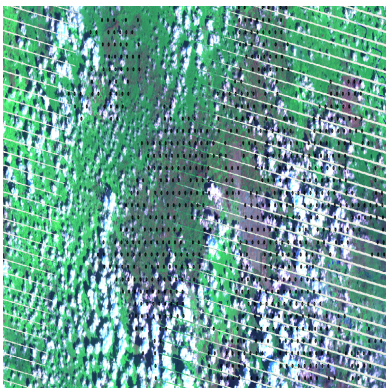

(b) After fire event.

Figure 2: Figure shows the Landsat multispectral image composites before and after a large fire event in Brazil, South America that is detected by RAPT algorithm but missing in MCD64A1. The dots correspond to the center of a 500 m. MODIS pixel. The post-event composite image shows a clear burn scar, which is in good agreement with the spatial boundary of burned pixels detected by the algorithm. Figure best viewed in color.

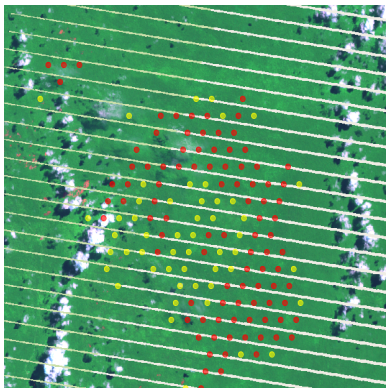

(a) Before fire event.

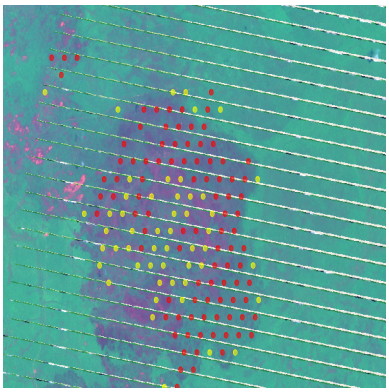

(b) After fire event.

Figure 3: Figure shows the before and after Landsat multispectral image composities corresponding to a large fire event in Indonesia that is detected by RAPT algorithm but missing in MCD64A1. The post-event composite image shows a clear burn scar, which is in good agreement with the spatial boundary of burned pixels detected by the algorithm. Figure best viewed in color.

Manual inspection of false color image composites of Landsat data is commonly used to verify the accuracy of a burned area product. We carefully examined a number of fire events detected by RAPT in the tropical forests for which clear Landsat images were available both before and after the event. In most of these cases, we are able to see a burn scar in the post-fire composites. As an illustration, in Figures 2 and 3 we show Landsat false color composites of two large fire events in Brazil and Indonesia, respectively. The dots shown in each image correspond to the center of a 500 m pixel that is detected by RAPT scheme as burned (note that these events were missing in the MCD64A1 burned area product). The Figures clearly show a good agreement between the RAPT detection and the burn scar in the "after event" images, while there is evidence of a healthy forest cover in the "before event" images. This approach does not provide a comprehensive validation, as manual inspection of every identified burn event will be extremely time consuming. Furthermore, manual inspection is particularly challenging to use in the tropics where it is difficult to find cloud free images.

4.2 Manual inspection of vegetation index time series

Fire events often reduce the total leaf cover of a pixel and are therefore visible in vegetation index time series as a sudden drop in vegetation index followed by a gradual recovery. Though, vegetation index can go down for a number of other reasons unrelated to fire, but a synchronized drop in vegetation for a spatially contiguous set of locations increases our confidence that they are associated with fire, especially when active fire hotspots are present in some

of the locations. Hence, one way to validate fire events detected by RAPT is to check if the time of the event is associated with a sudden synchronized drop in vegetation index. As an illustration, Figure 4c shows the temporal profile of the enhanced vegetation index (EVI) corresponding of a typical burned pixel in Indonesia. The vegetation time series shows an abrupt change in year 2006 followed by a gradual recovery. Figure 4d shows the EVI profiles of all pixels belonging to a fire event for a specific date. We observe that all these pixels show a synchronized vegetation loss on the same date. Such sudden synchronized drops in vegetation at the time of event is visible for a vast majority of locations detected by RAPT, as can be easily seen in the publicly available viewer.

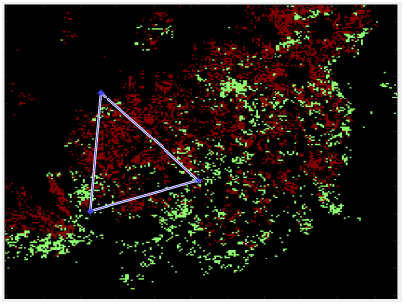

(a) Quality map by MCD64A1 (*red* is bad quality, *green* is good quality)

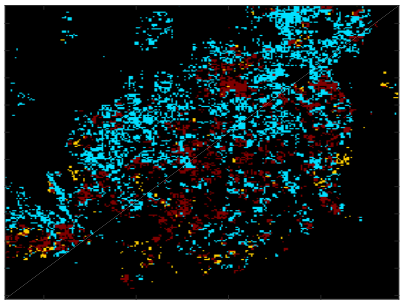

(b) Comparison map (*blue* is only RAPT, *red* is common, *yellow* is only MCD64A1)

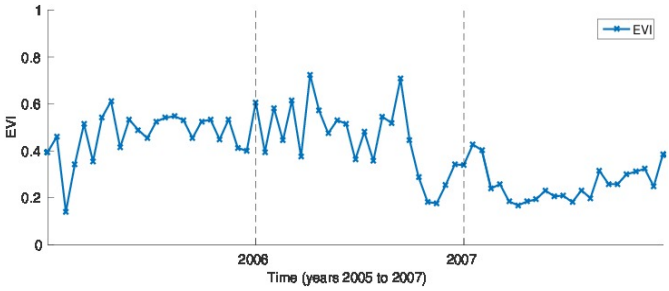

(c) EVI profile of a single burned pixel.

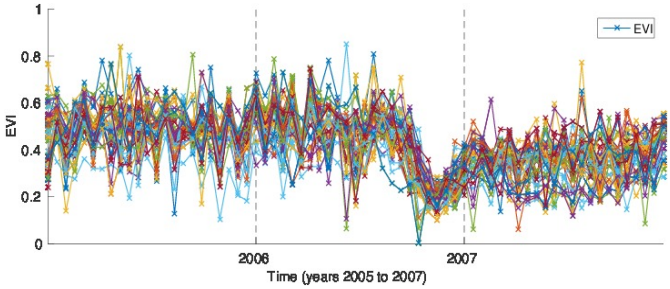

(d) EVI series of a fire event.

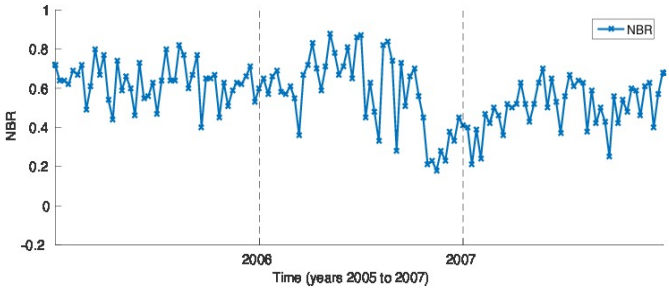

(e) NBR profile of a single burned pixel.

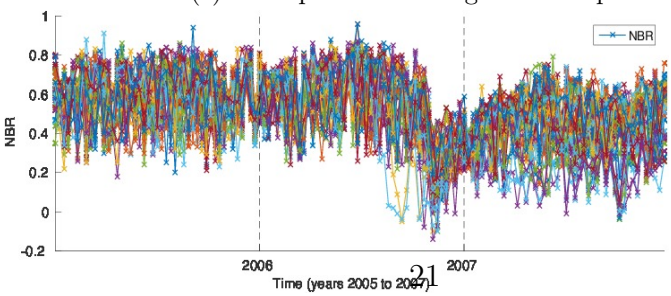

(f) NBR series of a fire event.

Figure 4: Figure shows a region in Indonesia where MCD64A1 missed several burned pixels due to poor data quality around burn date. The evidence from (i) EVI time series and (ii) NBR series indicates that the additional burned pixels identified by RAPT are true burns.

4.3 Validation using Normalized Burn Ratio on Landsat Images

A commonly used approach for quantitative evaluation of burned area products is to use independent statistics such as Normalized Burn Ratio (NBR) on Landsat images to derive validation data. Specifically, a validation label (burn/ no burn) is assigned to each pixel in the region of study for a particular year using NBR data. The validation labels are then used to compute evaluation measures such as user's and producer's accuracy for the burned area products being evaluated.

Typically, the methodology to construct validation labels for a Landsat tile from NBR involves the following steps. First, a time interval (typically a fire season) is chosen for which the validation labels are to be derived. Next, a post-burn image is selected that shows a burn scar in its Landsat false color composite image and is also relatively clear of clouds and other quality issues. Once the post-burn image is determined, a cloud free pre-burn image is selected in the previous year for the same season as the post-burn image. Selecting the pre-burn image from the same season reduces differences arising due to the seasonal variations in spectral values of the land surface. Then the differenced NBR (dNBR) value of each pixel is computed by taking the difference between the NBR values of the pixel on the selected pre-burn and post-burn dates. Finally, a decision threshold on the dNBR score is selected and the pixels with dNBR value greater than this selected threshold are considered as burned in the validation data and remaining are considered as unburned (Giglio et al. (2009)). Selection of this threshold is done via visual

inspection of Landsat false color composite images such that the burned locations in the resulting validation data best match with the scar visible in the Landsat composite. The obtained validation data is used to compute the user's and producer's accuracy for the burned area product being evaluated.

This approach is difficult to use for a comprehensive evaluation of burned products in the tropics due to the following three reasons. First, this approach is not very effective in the tropics because reasonable quality post-burn Landsat images are often not available close to the date of the event either due to cloud cover or due to smoke from fires. In fact, for many fire events a clear Landsat image is often not available for an entire year, making the scar to go away or become less visible with time. This is possibly why none of the burned area products have been quantitatively evaluated in the tropics to the best of our knowledge. Second, this approach requires considerable human effort to select pre-burn and post-burn images, and decision threshold on dNBR for each Landsat tile. This makes it cumbersome for evaluating large regions (eg. several hundred Landsat tiles). Third, in this approach evaluation is performed only on Landsat tiles that have some fire activity reported by the product being evaluated- making it harder to assess omission errors of the product in case the entire burn event in the Landsat tile was missed by the product.

4.4 Validation using Normalized Burn Ratio on the scale of MODIS tile

Here we present a MODIS-based validation strategy for evaluating burned area products. This strategy addresses the issue of poor data quality of Landsat images in tropics, while also reducing the requirements on human supervision. As a result, the scheme enables us to present a comprehensive quantitative evaluation of burned area products in the tropics.

4.4.1 Constructing a MODIS-based validation data

We use the MODIS-based burn index computed from the band 2 and band 7 of multispectral reflectance data. This index approximately corresponds to the Normalized Burn Ratio developed in context of Landsat band 4 (Near Infra-Red) and band 7 (Short Wave Infra-Red) (Loboda et al. (2007)). MODIS-derived NBR is relatively less impacted by data quality issues observed in Landsat-based validation because MODIS product uses composites of daily images compared to 16-day observations from Landsat. Using daily composites is especially helpful in the tropics where finding clear images around the event date is difficult.

$$NBR = \frac{band2 - band7}{band2 + band7}$$

$$dNBR = NBR_{prefire} - NBR_{postfire}$$

Though MODIS-based NBR is less impacted by data quality issues than

their Landsat-based counterparts, it is still challenging to use MODIS-based NBR to derive validation data set. Due to the larger size of a MODIS tile compared to a Landsat tile, a single MODIS tile often has multiple fire events that are associated with different burn dates. For each event, the dNBR signal is strongest at the actual date of event and can fade away if computed on a date farther away from the event date. Thus, selecting a single event date for the entire MODIS tile is not effective. In order to address this issue, we select the expected event date for each pixel so that dNBR is computed with respect to these event dates. Moreover, this selection has to be done without human supervision for this approach to scale for large regions. In our approach, we make use of active fire hotspots as a heuristic to guide the selection of expected event date for pixels. In particular, we select the expected event date for a pixel based on the date associated with the spatially nearest active fire hotspot in that same year. If there are multiple active fire hotspots observed in the same year, we chose the first occurrence (as it corresponds to the start of the fire). For the burned pixels, the selected event date is likely to correspond to the actual burn date. For the unburned pixels, there is no actual burn date, and the selected date is one in the fire season of the spatial region.

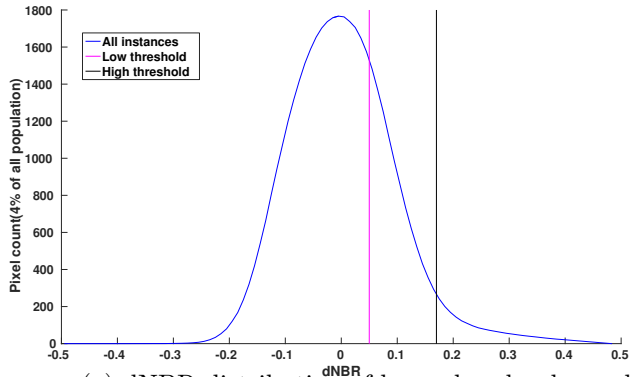

(a) dNBR distribution of burned and unburned pixels.

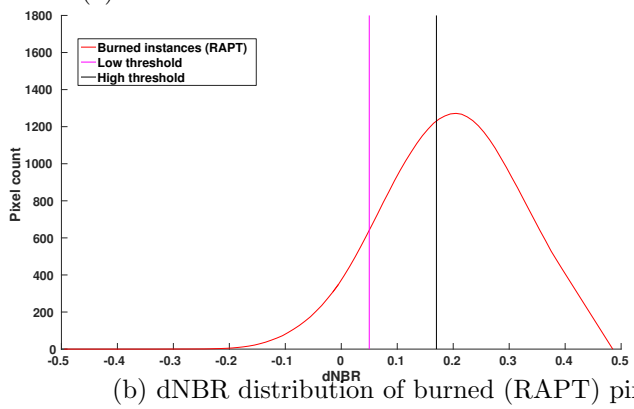

(b) dNBR distribution of burned (RAPT) pixels.

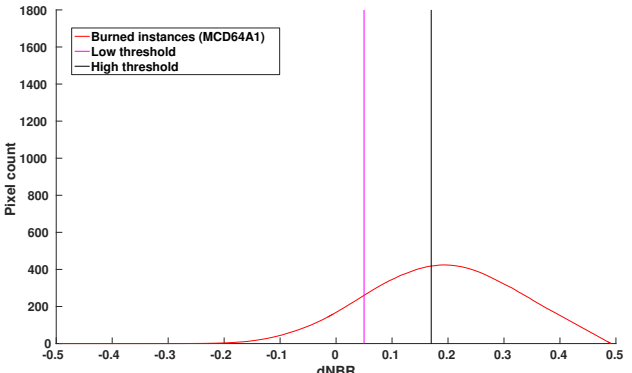

(c) dNBR distribution of burned (MCD64A1) pixels.

Figure 5: dNBR distributions for (i) all pixels, (ii) RAPT events and (iii) MCD64A1 events for MODIS tile h29v09 for year 2006.

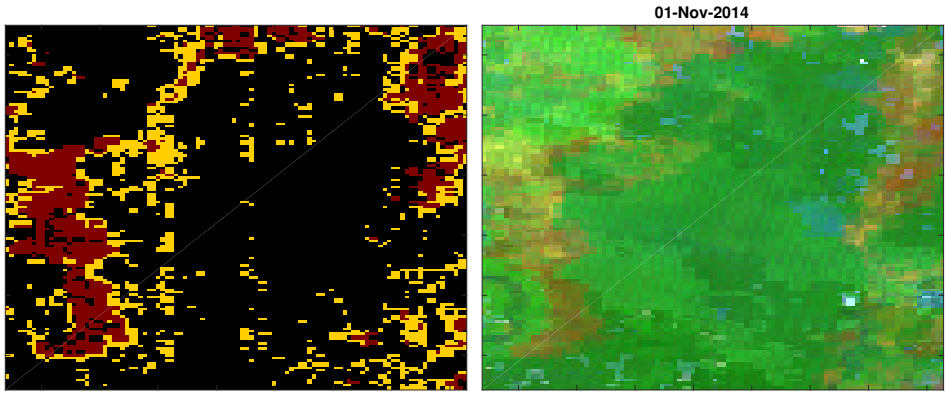

(a) dNBR generated validation labels- burned pixels (*red*), unburned pixels (*black*) and eliminated pixels (*yellow*).

(b) False Color Composite from MODIS multispectral data. The burned areas are visible as red patches.

Figure 6: An illustrative example of validation labels derived using MODIS-dNBR.

Next, a post-burn NBR value has to be associated with each pixel with respect to the event date associated with it for the given year. One possible approach is to use the NBR value for the expected event date or the next date since the burn scar is expected to be the strongest immediately after the burning. However, the spectral observations on these dates are also likely to be most impacted by quality issues due to smoke from fires. Since the burn scar fades as we go farther away from the event date, as a trade-off we use the median NBR value of the 8 time steps (approximately 2 months) after the associated event date for each pixel. We have noticed that in most places in tropics, scars tend to last for two months and using the median value brings robustness to any poor quality data.

To assign a pre-burn NBR, one possibility was to take the median from 8 time steps of the same season in the previous year. This works in practice in

most parts of the world. However, in tropics we observed that a large number of locations show multiple burns in consecutive years (eg. when preparing land for deforestation). In such scenario using the previous year leads to a lower difference for the burns in years following the first burn event. To minimize this problem, in our approach we use the median NBR value of the 8 time steps for same season from the first four years (2001-2004) instead of the previous year, and therefore the dNBR-based validation is performed only for 2005 onward. (Note that there may still be some pixels that are burned in 2001-2004, and thus could impact the evaluation results if these are burned in future years.)

The differenced NBR is computed by taking the difference between the assigned pre-burn and post-burn NBR values. The final task is to determine a decision threshold on dNBR scores to create the validation labels. Note that MODIS-based dNBR has greater confusion between burned and unburned pixels compared to Landsat dNBR due to its coarser spatial resolution and the nature of its reflectance bands. This combined with the fact that a single MODIS tile may have many fires on multiple dates, makes it infeasible to determine this threshold even with careful manual inspection. We noticed that pixels with a high dNBR value typically show signs of a burn event, while pixels with a low dNBR value do not. Hence, for pixels with extreme values of dNBR, it is possible to assign a validation label with high certainty. As an illustration, Figures 5b and 5c show the dNBR distribution of burned and unburned pixels assigned by RAPT and MCD64A1. But, there is an interval of dNBR values in which there is confusion in the actual label. Thus, we observe that there exists a range of dNBR values, th_{low} and th_{high}, such that

pixels with dNBR greater than th_{high} can be marked as burned and pixels with dNBR lower than th_{low} can be marked as unburned in the validation labels with reasonable certainty.

To avoid penalizing algorithms for either identifying or missing pixels belonging to this high confusion dNBR region, we exclude these pixels from our validation data set. As an illustration, Figure 5c shows the pixels assigned to burned class in validation set in *red*, to unburned class in *black*, and those eliminated from evaluation in *yellow* for a sample region. We observe that some of the eliminated pixels form the boundaries of large fire events (and therefore may correspond to partial burning) while others belong to unburned regions. Thus, by eliminating these pixels we also reduce the impact of edge effects introduced by coarse resolution data sets, where a burned MODIS pixel at the edge of a fire scar often covers a combination of burned and unburned areas.

For most tiles, it is desirable to keep the width of the threshold window (th_{low} and th_{high}) to be small, as it is possible to artificially increase user's and producer's accuracy by considerably increasing this window and evaluating only on a small number of instances. Ideally, the threshold window also needs to be adapted for different tiles (and in fact for different regions within a MODIS tile) to account for the diversity of spectral signal. However, adapting the threshold window for each spatial region would require significant human effort. In our evaluation, we used a single threshold window of $th_{low} = 0.05$ and $th_{high} = 0.17$ that appeared reasonable for all tiles being evaluated. To ensure a reasonable validation set, we constrained the threshold selection such that no more than 20% of the total burned pixels for both RAPT and

MCD64A1 are excluded for each of the tiles in the tropics on which we performed evaluation.

4.4.2 Results of MODIS-dNBR evaluation

The dNBR-derived validation data set enables a comprehensive validation by estimating the user's and producer's accuracy for the fires detected by RAPT from 2005 to 2014 for each MODIS tile in the region of study. (No validation labels is available between 2001-2004 since our dNBR computation requires first four years for building pre-burn NBR value). Table 2 reports the user's and producer's accuracy for both RAPT and MCD64A1 for each tile in our region of study. Our first observation from Table 2 is that both RAPT and MCD64A1 show a high user's accuracy, i.e. they do not have many spurious burn events (see the first and third column of table). Table 2 also shows that RAPT has a considerably higher producer's accuracy than MCD64A1 (almost three times on an aggregate level). Note that from the results in Table 2 it appears that the producer's accuracy, even for RAPT, is low (between 0.18 to 0.54). A part of it explained by sources of errors of omission, which are discussed in detail in Section 5. However, we noticed that a significant loss in producer's accuracy is an artifact of using dNBR-based validation labels. dNBR is a surrogate signal that is being used to derive validation labels, and some unburned pixels may show a high dNBR by random chance. These unburned pixels get incorrectly assigned to burned class in the validation labels, and hence artificially reduce the estimates of producer's accuracy.

The higher producer's accuracy of RAPT relative to MCD64A1 can be at-

Table 2: Table shows the user's and producer's accuracy of RAPT and MCD64A1 products for each tile in the region of study.

MODIS	RAPT		MCD64A1	
tile	User's acc.	Producer's acc.	User's acc.	Producer's acc.
h11v09	0.90	0.54	0.94	0.10
h12v09	0.95	0.54	0.99	0.17
h11v10	0.95	0.40	0.96	0.18
h12v10	0.98	0.29	0.98	0.19
h13v09	0.88	0.51	0.99	0.09
h28v08	0.99	0.31	0.91	0.08
h29v08	0.99	0.18	0.58	0.02
h28v09	0.99	0.34	0.91	0.13
h29v09	0.93	0.47	0.84	0.18

tributed to two reasons. First, the burned area algorithm to derive MCD64A1 product uses several hand-crafted rules and parameters for obtaining training samples from active fire hotspots as well as keeping commission errors low. These manually determined thresholds of MCD64A1 appear to be too conservative for the tropical forests, which has been validated (Giglio et al. (2009)) to have high producer's accuracy in areas outside tropics, but not in tropical forests. In contrast, RAPT algorithm automatically builds a model for each spatial region (MODIS tile) and land class such that it jointly maximizes the user's and producer's accuracy, and hence is able to build a good model for different areas in the tropics without facing the limitations of expert-specified rules and parameter tuning. Second, MCD64A1 uses daily data and detects fires based on vegetation change in 20 days around the date of the fire event. We noticed that there are several gaps in MCD64A1 burned areas due to lack of high quality surface observations, i.e. it excludes pixels with poor data quality in a 20 day period. This problem is particularly relevant for tropical

areas with high average percent cloud cover and where burning results in the release of large quantities of particulate matter into the atmosphere. In contrast, RAPT is less impacted by poor data quality because it uses a longer temporal context to identify fire scars that sometimes remain detectable for multiple months. As an illustration, Figure 4b shows the additional burned pixels (in *blue*) identified by RAPT in a region in Indonesia. Figure 4a shows the map of burned pixels (RAPT union MCD64A1) that were classified as unburned by MCD64A1 due to poor quality observations on their respective burn dates. The Figure shows that a large fraction of burned pixels identified by RAPT but missing in MCD64A1 were assigned to unburned class due to a poor data quality issue on the burn date. The Figure 4 also shows a typical EVI and NBR profile of a pixel assigned to burned class by RAPT in the *triangle region*. We can clearly see a sharp decrease followed by a gradual recovery in these signals, which is a signature of fire event, thus suggesting that these additional burned pixels identified by RAPT are true burns that are missed by MCD64A1 due to poor data quality at the time of burn event.

5 Limitations of our burned area detection

In this section we discuss the major limitations of RAPT burned area mapping framework that we observed in the tropical forests.

5.1 Errors of commission

We are able to validate most of the high confidence events detected by RAPT using one or more lines of evidence. However, RAPT does identify locations

that appear to be incorrectly labeled as burn events. Our manual investigation that many of these errors of commission occur in locations for which the MODIS land classification product MOD12Q1 appears to be uncertain regarding their land cover (i.e., classified as forests in some years and non-forests in other years). One possible explanation for higher commission errors in these locations is that many of these locations are not forests; hence, RAPT algorithm trained for forest class performs poorly on these pixels belonging to a different land class (such as grasslands, shrubs, wetlands). Note that there are far more errors of commission made in Stage 1, but most of those get corrected in subsequent stages that impose constraints on spatial proximity of active fire hotspots and length of the temporal window in which burn scar is visible. To minimize errors of commission due to incorrect MODIS label, in Section 4 we have only presented results for those pixels that are labeled as forest by MODIS MOD12Q1 consecutively from 2001-2004.

5.2 Errors of omission

Errors of omission are particularly hard to quantify in the absence of a ground truth. But from Table 1 and 2, it is obvious that RAPT missed many pixels that are identified as burned by MCD64A1 (Table 1) or show a large dNBR value (Table 2). Our careful investigation identified a number of possible reasons for these omission errors.

One major reason for omission errors is the absence of any Active fire hotspot in the spatial proximity of burned pixels (even though a burn scar was detected on these pixels in RAPT Stage 1). However, the exclusion of

these pixels is necessary since the scar classifier if used without co-occurrence of active fire will have many errors of commission.

Another major source of omission errors is due to the constraint that the burn scar must be visible according to RAPT stage 1 in at least 4 consecutive time steps. In fact, for most of the locations identified as burned by MCD64A1 but not by RAPT (see last column of Table 1), we noticed that RAPT stage 1 detects burn scar in one or more time steps. But we have chosen to exclude locations for which RAPT identifies burn in less than 4 consecutive time steps, as many of them are difficult to validate using any line of evidence.

Finally, a small fraction of omission errors correspond to burned pixels for which the scar classifier did not detect any burn scar in the year. One possible explanation for the absence of burn scar is that the classifier is not able to model all the variations of burn scars due to the lack of representative training samples in presence of multi-modality.

5.3 Fires in locations with high uncertainty in forest label

RAPT identified burned areas in 9 out of 15 MODIS tiles in the region of study. In the excluded MODIS tiles, the RAPT algorithm does not report any burned areas because it was not able to build a classification model in stage 1 to identify burn scars in forests with a reasonable user's accuracy. This situation can arise if the spectral features being used for building models are not discriminative or if the classifier (logistic regression in our case) is

not appropriate to model the decision boundary.

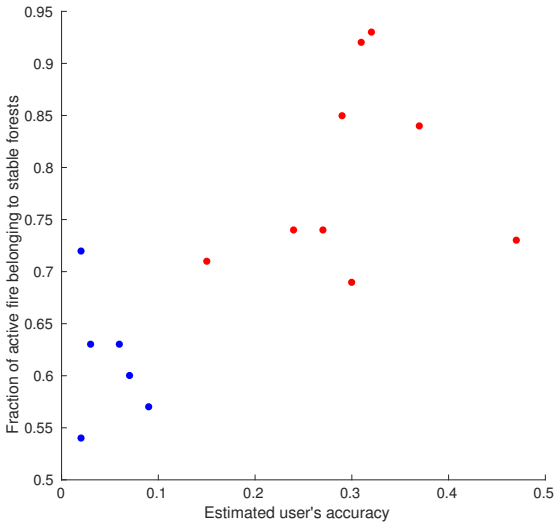

Figure 7: Figure shows the relationship between number of observed active fire pixels in stable forests versus the user's accuracy estimated by RAPT for included tiles (in red) and excluded tiles(in blue).

After careful investigation of the reason behind this issue, we identified an interesting relationship between the user's accuracy of RAPT stage 1 and the stability of the MODIS forest class labels of a tile. Specifically, we noticed that in the 6 excluded tiles the active fire hotspots occurred in locations that exhibit a high uncertainty in their land cover labels according to MODIS land cover classification product. Figure 7 shows the relationship between the estimated lower bound on user's accuracy of Stage 1 classifier and the stability of forest class in pixels with active fire hotspots. For each MODIS tile the x-axis corresponds to the estimated lower bound on the user's accuracy of Stage 1 classifier and the y-axis corresponds to the fraction of the active fire hotspots which belong to stable forests (i.e. had MODIS land cover label as forest in all 5 years before the year of active fire). Due to the

limitations of the MODIS land cover classification product, some of the pixels belonging to non-forest land classes or mixture of forest and non-forest land classes are also present in the MODIS forest land cover class The current implementation of RAPT is impacted by such errors in land cover labels and additional work is needed to train classification models for such tiles.

6 Burning associated with forest conversions

Large-scale plantations often do not comply with regulations for deforestation and employ cost-effective but environmentally damaging slash-and-burn practices for clearing forested areas. A timely-updated, reliable burned area product can be helpful in identifying such illegally constructed plantations. In this section we report the co-occurrence of fire activity in forested locations that exhibited signs of a land cover conversion. The MODIS land cover classification product MOD12Q1 is used to identify a set of pixels with signs of land cover conversion in each MODIS tile. In particular, a pixel is considered to have been converted from a forest class to non-forest class if it is labeled as forest in the years between 2001-2003 and labeled as non-forest in the years between 2010-2012. Table 3 reports the number of converted pixels identified by the above heuristic in each tile. A converted pixel is considered to be associated with burn activity according to a given burned area product if the product reported a burn event between 2004-2009. Table 3 reports the percent of converted pixels associated with a burn event according to the RAPT and MCD64A1 products in each MODIS tile.

We notice that MCD64A1 has only a small percentage of converted pix-

Table 3: Table reports number of converted pixels in each MODIS tile between 2004 to 2009 and the percentage of these converted pixels associated with a burn activity by RAPT and MCD64A1.

tile	converted pixels	% RAPT(high)	% MCD64A1
h11v09	10021	96	47
h12v09	51628	81	33
h11v10	26134	74	30
h12v10	82936	62	37
h13v09	41527	53	05
h28v08	24788	35	11
h29v08	11041	35	05
h28v09	28943	24	08
h29v09	17219	46	08

els associated with a fire activity. We attribute this to the poor producer's accuracy of MCD64A1 in the tropics. In contrast, the RAPT product shows a significantly higher occurrence of fire among the converted pixels. As an illustration, Figure 8 shows the Google Earth image of a region in Amazon that experienced several deforestation events between 2002 and 2015. Figure 8 also shows the burn events identified by RAPT in this region (as *yellow* and *red* circles representing pixel centers). The RAPT detection shows a considerable agreement with the deforestation patches (visible in Google Earth imagery in 2015), suggesting a rampant use of burning to clear forested areas in this region. In fact, we observed that for a typical converted pixel in this region, the burn events often occured in multiple years before the pixel got converted completely to a non-forest land class (i.e. got labeled by MODIS as non-forest land cover). These results suggest that a regularly updated fire product like RAPT can play a crucial role in early warning systems to monitor active deforestation fronts for preventive intervention.

Figure 8: Figure shows the RAPT events detected between 2002 and 2014 for a region in Amazon that also experienced significant deforestation activity. We notice that the RAPT detections show a good agreement with the visible deforested patches, while the RAPT detections also identified in MCD64A1 cover only a small portion of deforested area. The Figure also shows the number of RAPT events (burns in different years) between this period. We notice that a majority of burned pixels have experienced 3 or more burn events. The figure also shows the burn events and MODIS land cover sequence for a typical burned pixel in this region. We notice that for this representative pixel a sequence of 3 consecutive burn events is followed by a land cover conversion from forest to non-forest in MODIS.

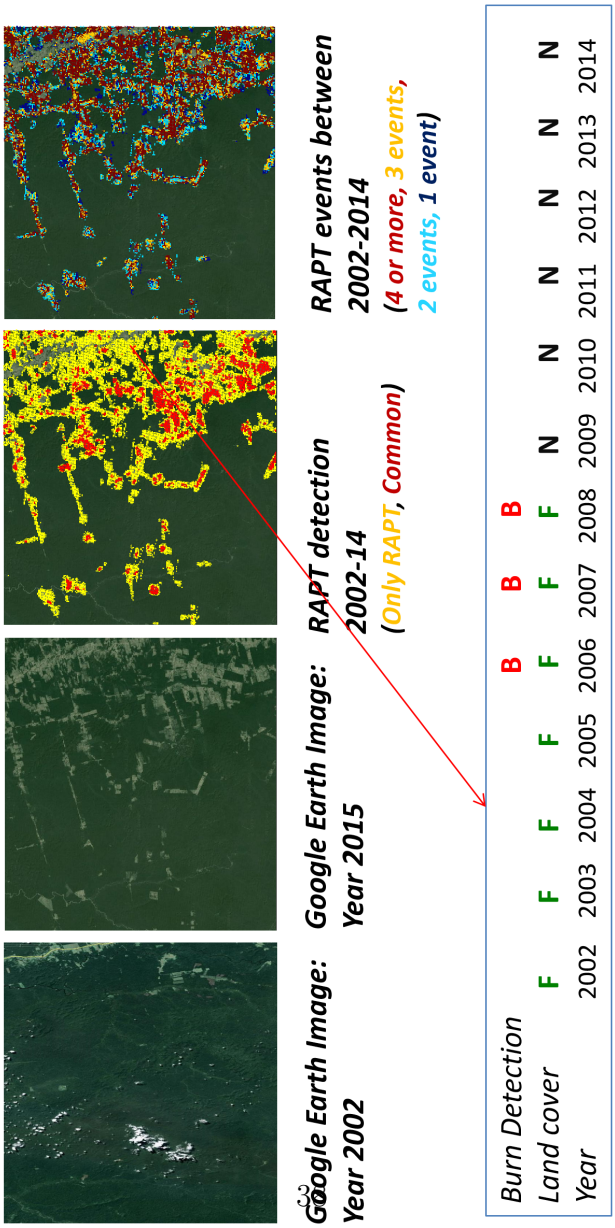

7 Concluding remarks

We presented results on a new MODIS-based burned area product that has comparable user's accuracy but considerably better producers's accuracy compared to the state-of-art MCD64A1 in the tropical forests. Though there is considerable uncertainty in translating burned area into carbon emissions, the significantly larger burned area identified by RAPT will help addressing the current uncertainties in tropical carbon budgets. Moreover, this product can be used to identify and mitigate practices such as slash-and-burn that are often used to illegally clear forested locations for plantations and other commercial activity.

Even though RAPT results are in the tropical forests of Amazon and South-east Asia, the algorithm offers opportunities for global-scale fire mapping. Since, the presented algorithm does not rely on hand-crafted rules or parameters, and automatically adjusts its model parameters to the specifics of different spatial regions and land cover classes, it can be adapted to identify burned areas in other land classes and geographical regions.

In the RAPT framework, the predictive model is trained on homogeneous land cover and geographical regions. The presented implementation of RAPT uses MODIS tile boundaries to address geographical heterogeneity and relies on the MODIS land classification for a good quality forest mask. However, there may be considerable variability within a MODIS tile, and the MODIS land cover labels are coarse (many sub-classes) and may also be incorrect. The ability of the RAPT framework to identify fires with high accuracy is impacted by these issues. Hence, further extensions of this framework are

needed that can perform automated data-driven grouping of pixels, instead of relying on land classification products and MODIS tile boundaries.

Acknowledgement This research was supported in part by the University of Minnesota Doctoral Dissertation Fellowship, National Science Foundation under Grants IIS-1029711 and IIS-0905581, and NASA grant NNX12AP37G. Access to computing facilities was provided by the University of Minnesota Supercomputing Institute.

References

Bastarrika, A., Chuvieco, E., and Martín, M. P. (2011). Mapping burned areas from landsat tm/etm+ data with a two-phase algorithm: Balancing omission and commission errors. *Remote Sensing of Environment*, 115(4):1003–1012.

Chen, Y., Randerson, J. T., Morton, D. C., DeFries, R. S., Collatz, G. J., Kasibhatla, P. S., Giglio, L., Jin, Y., and Marlier, M. E. (2011). Forecasting fire season severity in south america using sea surface temperature anomalies. *Science*, 334(6057):787–791.

Fraser, R. H., Li, Z., and Cihlar, J. (2000). Hotspot and NDVI Differencing Synergy (HANDS): a new technique for burned area mapping over boreal forest. *Remote Sensing of Environment*, 74(3):362–376.

Friedl, M. A., McIver, D. K., Hodges, J. C., Zhang, X., Muchoney, D., Strahler, A. H., Woodcock, C. E., Gopal, S., Schneider, A., Cooper, A.,

et al. (2002). Global land cover mapping from modis: algorithms and early results. *Remote Sensing of Environment*, 83(1):287–302.

Fuller, D. and Fulk, M. (2001). Burned area in kalimantan, indonesia mapped with noaa-avhrr and landsat tm imagery. *International Journal of Remote Sensing*, 22(4):691–697.

Giglio, L., Loboda, T., Roy, D. P., Quayle, B., and Justice, C. O. (2009). An active-fire based burned area mapping algorithm for the modis sensor. *Remote Sensing of Environment*, 113(2):408–420.

Giglio, L., Van der Werf, G., Randerson, J., Collatz, G., and Kasibhatla, P. (2006). Global estimation of burned area using modis active fire observations. *Atmospheric Chemistry and Physics*, 6(4):957–974.

Koutsias, N. and Karteris, M. (1998). Logistic regression modelling of multitemporal thematic mapper data for burned area mapping. *International Journal of Remote Sensing*, 19(18):3499–3514.

Loboda, T. and Csiszar, I. (2007). Reconstruction of fire spread within wildland fire events in northern eurasia from the modis active fire product. *Global and Planetary Change*, 56(3):258–273.

Loboda, T., O'Neal, K., and Csiszar, I. (2007). Regionally adaptable dNBR-based algorithm for burned area mapping from MODIS data. *Remote Sensing of Environment*, 109(4):429–442.

Minko, N. P. (2000). The atmospheric impact of boreal forest fires in far eastern siberia on the seasonal variation of carbon monoxide: Observations

at rishiri, a northern remote island in japan. *Geophysical Research Letters*, 27(24):4073–4076.

Mithal, V., Nayak, G., Khandelwal, A., Kumar, V., Oza, N., and Nemani, R. (2016). RAPT: Rare class prediction in absence of true labels. Under submission, University of Minnesota.

Pu, R. and Gong, P. (2004). Determination of burnt scars using logistic regression and neural network techniques from a single post-fire landsat 7 etm+ image. *Photogrammetric Engineering & Remote Sensing*, 70(7):841–850.

Pu, R., Gong, P., Li, Z., and Scarborough, J. (2004). A dynamic algorithm for wildfire mapping with noaa/avhrr data. *International Journal of Wildland Fire*, 13(3):275–285.

Randerson, J., Chen, Y., Werf, G., Rogers, B., and Morton, D. (2012). Global burned area and biomass burning emissions from small fires. *Journal of Geophysical Research: Biogeosciences (2005–2012)*, 117(G4).

Roy, D. P., Giglio, L., Kendall, J. D., and Justice, C. O. (1999). Multi-temporal active-fire based burn scar detection algorithm. *International Journal of Remote Sensing*, 20(5):1031–1038.

Schultz, M. (2002). On the use of atsr fire count data to estimate the seasonal and interannual variability of vegetation fire emissions. *Atmospheric Chemistry and Physics*, 2(5):387–395.

Senator, T. E. (2005). Multi-stage classification. In *ICDM*, pages 386–393.

780 Smith, A., Lentile, L., Hudak, A., and Morgan, P. (2007). Evaluation of
781 linear spectral unmixing and δnbr for predicting post-fire recovery in a
782 north american ponderosa pine forest. *International Journal of Remote*
783 *Sensing*, 28(22):5159–5166.

784 Sukhinin, A. I., French, N. H., Kasischke, E. S., Hewson, J. H., Soja, A. J.,
785 Csiszar, I. A., Hyer, E. J., Loboda, T., Conrad, S. G., Romasko, V. I.,
786 et al. (2004). Avhrr-based mapping of fires in russia: New products for fire
787 management and carbon cycle studies. *Remote Sensing of Environment*,
788 93(4):546–564.

789 Vermote, E., Kotchenova, S., and Ray, J. (2011). Modis surface reflectance
790 user's guide. *MODIS Land Surface Reflectance Science Computing Facility,*
791 *version*, 1.